Neuropharmacology 77 (2014) 453–464

Contents lists available at ScienceDirect

Neuropharmacology

journal homepage: www.elsevier.com/locate/neuropharm

Recombinant human thioredoxin-1 promotes neurogenesis and facilitates cognitive recovery following cerebral ischemia in mice

Li Tian [a,1], Huang Nie [a,1], Yang Zhang [b,1], Yu Chen [a], Zhengwu Peng [c], Min Cai [a], Haidong Wei [a], Pei Qin [a], Hailong Dong [a,**], Lize Xiong [a,*]

[a] Department of Anesthesiology, Xijing Hospital, The Fourth Military Medical University, 127th Changle West Road, Xi'an 710032, China
[b] Department of Orthopedic Surgery, Xijing Hospital, The Fourth Military Medical University, Xi'an 710032, China
[c] Department of Psychosomatic Medicine, Xijing Hospital, The Fourth Military Medical University, Xi'an 710032, China

ARTICLE INFO

Article history:
Received 1 December 2012
Received in revised form
18 October 2013
Accepted 23 October 2013

Keywords:
Recombinant human Trx-1
Cerebral ischemia
Hippocampus
Neurogenesis
Learning and memory
ERK signaling pathway

ABSTRACT

Cerebral ischemia (CI) can induce loss of hippocampal neurons, causing cognitive dysfunction such as learning and memory deficits. In adult mammals, the hippocampal dentate gyrus contains neural stem cells (NSCs) that continuously generate newborn neurons and integrate into the pre-existing networks throughout life, which may ameliorate cognitive dysfunction following CI. Recent studies have demonstrated that recombinant human thioredoxin-1 (rhTrx-1) could promote proliferation of human adipose tissue-derived mesenchymal stem cells and angiogenesis. To investigate whether rhTrx-1 also regulates hippocampal neurogenesis following CI and its underlying mechanisms, adult mice were subjected to bilateral common carotid arteries occlusion (BCCAO) to induce CI and treated with rhTrx-1 before reperfusion. Mice treated with rhTrx-1 showed shortened escape latencies in Morris water maze by 30 days and improvements in spatial memory demonstrated by probe trial test. Enhanced NSCs proliferation was observed at day 14, indicated by BrdU and Ki67 immunostaining. Doublecortin $(DCX)^+$ cells were also significantly increased following rhTrx-1 treatment. Despite increases in $BrdU^+/NeuN^+$ cells by day 30, the double-labeling to total $BrdU^+$ ratio was not affected by rhTrx-1 treatment. The promotive effects of rhTrx-1 on NSCs proliferation and differentiation were further confirmed in *in vitro* assays. Western blot revealed increased ERK1/2 phosphorylation after rhTrx-1 treatment, and the ERK inhibitor U0126 abrogated the effects of rhTrx-1 on NSCs proliferation. These results provide initial evidence that rhTrx-1 effects neurogenesis through the ERK signaling pathway and are beneficial for improving spatial learning and memory in adult mice following global CI.

© 2013 The Authors. Published by Elsevier Ltd. Open access under CC BY-NC-ND license.

1. Introduction

Cerebral ischemic (CI) and neurodegenerative diseases can induce hippocampal neuron loss of varying severity which are pivotally implicated in the deficiencies of spatial learning and memory (Bendel et al., 2005; Chen et al., 2000; Hartman et al., 2005; West et al., 1994). Although persistent progenitor cell proliferation and neurogenesis commonly follow ischemic periods in the forebrain subventricular zone and hippocampal dentate gyrus (DG), a phenomenon that has been well documented in rodent models, the definite role of neurogenesis following CI remains controversial.

Neurogenesis in response to ischemic neuron loss may be a result of neural stem cells (NSCs) participation in the endogenous repair processes of the adult mammalian brain (Okano et al., 2007). New neurons have been detected in the injured area of previously ischemic tissues, where these new cells were functionally integrated into existing cerebral circuits (Lichtenwalner and Parent, 2006). Conversely, neurogenesis has been suppressed using X-ray irradiation prior to bilateral common carotid arteries occlusion (BCCAO) in gerbil models, resulting in severe spatial learning and memory deficits following ischemia (Raber et al., 2004). These findings underscore the importance of neurogenesis in functional recovery. Enhanced hippocampal neurogenesis also facilitates long-

* Corresponding author. Tel.: +86 2984771262; fax: +86 83244986.
** Corresponding author. Tel.: +86 2984775337; fax: +86 2983244986.
E-mail addresses: hldong6@hotmail.com (H. Dong), mzkxlz@126.com, lxiong@fmmu.edu.cn (L. Xiong).
[1] These authors contributed equally to this work.

0028-3908 © 2013 The Authors. Published by Elsevier Ltd. Open access under CC BY-NC-ND license.
http://dx.doi.org/10.1016/j.neuropharm.2013.10.027

term potentiation and improves learning and memory (Abraham et al., 2002; Deng et al., 2010; Schmidt-Hieber et al., 2004). Therefore, facilitation of endogenous neurogenesis may be a promising regenerative strategy for ischemic stroke treatment.

Both direct and indirect approaches have been developed to stimulate proliferation and neurogenesis, attenuate infarct volume, and improve neurological deficits in the ischemic stroke model. Thioredoxin (Trx), a 12-kD oxidoreductase enzyme containing a dithiol-disulfide active site, is a redox-sensitive molecule with pleiotropic cellular effects involved in regulation of proliferation, redox states, and anti-apoptosis (Mukherjee and Martin, 2008). Two isoforms of Trx exist in mammalian cells. Cytosolic Trx-1, which can be translocated into the nucleus under certain circumstances, is the dominant form, and mitochondrial Trx-2 occurs relatively less frequently (Dunn et al., 2010). Endogenous Trx-1 production is induced by ischemia of brain tissues, where it is responsible for alleviation of oxidative damage. Moreover, exogenously administered recombinant human Trx-1 (rhTrx-1) can penetrate the blood brain barrier and exert a neuroprotective effect, as demonstrated in the middle cerebral artery occlusion (MCAO) model (Hattori et al., 2004). In addition to its role as an antioxidant, rhTrx-1 has also been reported to promote proliferation of human adipose tissue-derived mesenchymal stem cells and angiogenesis (Song et al., 2011; Welsh et al., 2002).

While the neuroprotective role of rhTrx-1 on injured neurons is well-established, rhTrx-1 may also promote neurogenesis and facilitate long-term recovery following CI. In order to investigate this hypothesis, the current study applied the BCCAO mouse model to investigate the role of rhTrx-1 in neurogenesis and its potential effect on cognitive deficits in learning and memory following global CI. In addition, the mechanisms associated with rhTrx-1 were tentatively explored.

2. Materials and methods

2.1. Animals and experimental design

Male C57BL/6J mice weighing 25–30 g purchased from the Laboratory Animal Center of the Fourth Military Medical University (Shaanxi, China) were used in the current *in vivo* studies. All experimental protocols complied with the *Guide for the Care and Use of Laboratory Animals* published by the National Institutes of Health (NIH). All experiments were also conducted in accordance with the Fourth Military Medical University Committee on Animal Care.

Mice were provided *ad libitum* access to food and water, and mice were housed in a temperature-controlled room with 12 h light–dark cycles. Experimental procedures for *in vivo* studies are described in Fig. 1. Briefly, mice were randomized into 3 groups: the sham-operated group, the cerebral ischemia plus vehicle (CI + Vehicle) group, and the cerebral ischemia plus rhTrx-1 (CI + rhTrx-1) group. Mice of each group were then equally divided into two subgroups for cognitive function evaluation and neurogenesis detection, respectively.

Mice of the CI + rhTrx-1 group were subjected to transient BCCAO for 20 min and intraperitoneal (i.p.) administration of rhTrx-1 containing 3 mg/kg of the cytosolic form of Trx (Sigma-Aldrich, St. Louise, MO) 10 min before reperfusion, according to the previously published method (Hattori et al., 2004; Tao et al., 2006). The CI + Vehicle group was simultaneously treated with similar BCCAO and i.p. administration of an equal volume of a 0.1 M phosphate buffered saline (PBS) solution as an inert vehicle (pH 7.4).

For neurogenesis analysis, mice were treated with daily 100 mg/kg i.p. injections of 5-bromo-2′-deoxyuridine (BrdU; Sigma-Aldrich, St. Louis, MO) for 4 consecutive days, during the peak of cell proliferation, or from days 9–12 after rhTrx-1 or vehicle treatment, according to the previously reported method (Bernabeu and Sharp, 2000; Liu et al., 1998). Mice of the sham-operated group also underwent i.p. injection of BrdU following sham surgeries. All the mice were sacrificed by days 14 and 30 and tissues were collected for further immunohistochemical study. Behavioral tests were performed 30 days after ischemia. NSCs were harvested from the fetal brain of pregnant Sprague-Dawley rats under deep anesthesia induced by treatment with 300 mg/kg i.p. chloral hydrate between embryonic days 14.5 and 16.5.

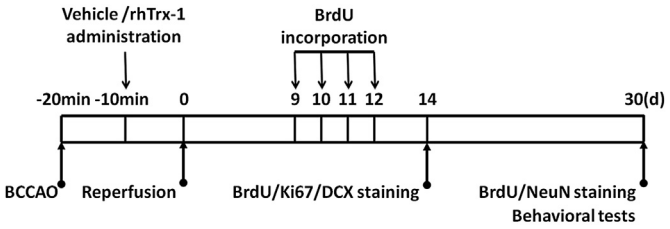

Fig. 1. Graphic presentation of the experimental protocol. The mice brain ischemia model was induced by BCCAO for 20 min. Experimental mice were randomized to receive either vehicle (0.1 M PBS, pH 7.4; i.p.) or an equal volume of rhTrx-1 (3 mg/kg; i.p.) 10 min before reperfusion. BrdU (100 mg/kg; i.p) was administrated daily for 4 consecutive days from 9 to 12 days after ischemia, and mice were then sacrificed for neurogenesis assays at 14 and 30 days post-ischemia. Behavioral testing was conducted 30 days after ischemia. Sham-operated animals were also injected with BrdU after sham surgeries and subjected to behavioral testing prior to sacrifice.

2.2. Transient forebrain cerebral ischemia

Mice were anesthetized with 2% isoflurane using a facemask, and CI was induced by transient BCCAO for 20 min, as described previously (Homi et al., 2003; Tajiri et al., 2004; Wu et al., 2001). Sham-operated animals were treated with the same surgical procedure, with the exception of occlusion. A PeriFlux System 5000 laser Doppler flowmeter (Perimed, Stockholm, Sweden) was used to measure regional cerebral blood flow (rCBF) from the start of anesthetic induction to 5 min after reperfusion (Olsson et al., 2004; Yoshioka et al., 2011). In the current experimental model, only results from mice with a mean CBF successfully reduced to 10% of the pre-ischemic value were used in subsequent data analysis. Rectal temperature was maintained at 37.5 ± 0.5 °C with a heating lamp until mice were revived.

2.3. Arterial blood gas determination

Left femoral arterial catheters were placed in separate groups of sham, CI + Vehicle and CI + rhTrx-1 groups ($n = 5$ in each group) to determine the arterial blood gas (Table. 1). About 0.2 ml of blood

Table 1
Physiologic parameters.

	T (°C)	pH	PaO_2 (mmHg)	$PaCO_2$ (mmHg)
Onset of BCCAO				
Sham	37.0 ± 0.12	7.39 ± 0.02	192.4 ± 0.8	37.5 ± 0.6
CI + vehicle	36.9 ± 0.20	7.40 ± 0.02	193.6 ± 1.1	38.1 ± 0.3
CI + rhTrx-1	37.1 ± 0.18	7.38 ± 0.04	189.5 ± 0.7	36.3 ± 0.4
Onset of reperfusion				
Sham	37.1 ± 0.15	7.41 ± 0.02	196.2 ± 0.5	39.1 ± 0.7
CI + vehicle	37.0 ± 0.11	7.40 ± 0.03	190.8 ± 1.6	38.5 ± 0.6
CI + rhTrx-1	37.1 ± 0.13	9.48 ± 0.04	192.9 ± 1.4	37.6 ± 0.5

Data was shown as mean ± SD. CI + vehicle and CI + rhTrx-1 mice were induced by transient BCCAO for 20 min, while sham-operated mice were treated with the same surgical procedure, with the exception of occlusion. BCCAO = bilateral common carotid arteries occlusion; PaO_2 = arterial oxygen tension; $PaCO_2$ = arterial carbon dioxide tension.

per mice was taken via femoral artery at the onset of BCCAO and reperfusion. After the final blood sample taken, blood gas was immediately analyzed (Rapidlab 1260, Bayer HealthCare, Uxbridge, United Kingdom).

2.4. Behavioral tests

Experimental C57BL/6J mice were subjected behavioral tests 30 days after ischemia. To minimize potential stress-related effects from previous behavioral performance testing, mice were first tested in the open field and then in the water maze, according to the previously published method (Raber et al., 2004).

2.4.1. Open-field test

Spontaneous locomotor activity was evaluated using an open-field test. Mice were individually placed in the center zone of an open field apparatus (50 × 50 × 40 cm). All movements were traced, and data were collected by video for 15 min after a 2 min habituation period. Total distances traveled and percentage of time spent in the 30 × 30 cm square center zone of the apparatus was analyzed by an automatic analyzing system (DigBehav, Jiliang Co. Ltd., Shanghai, China) (Miki et al., 2009; Miyakawa et al., 2001). The apparatus was cleaned with water after each trial.

2.4.2. Morris Water Maze (MWM) test

MWM was employed to assess mouse spatial learning and memory according to previously published methods (Morris, 1984; Rehni et al., 2009). The maze consisted of a large circular pool (150 cm in diameter, 45 cm in height, filled to a depth of 30 cm with water at 28 ± 1 °C). Water was made opaque with a white dye. A painted white platform (10 cm^2) was submerged and placed in the center of the target quadrant at 1 cm below the surface of water, providing the escape area. The position of the platform was maintained unaltered throughout the training session. Mice were allowed 4 training trials per day for 5 consecutive days. During each trial, mice were allowed to start from a random location in each of 4 quadrants. Mice were placed in a starting position in which its head was facing the wall, and the hidden platform was maintained in a fixed location. Each mouse was allowed a maximum of 60 s to find the submerged platform and rest for 30 s. If the mouse failed to find the hidden platform within 60 s, it was manually guided to the platform and allowed to rest for 30 s. The escape latency to find the hidden platform and the total path length to the platform were recorded. On the day 6, mice were subjected to a 60 s probe trial in which the platform was removed. The percentage of time spent in the target quadrant was considered to reflect memory retention, as previously described (Lai et al., 2007). A digital video camera was positioned directly above the water maze, enabling full collection of swim activity in the different quadrants, and the data feed was attached to a computer using DigBehav System (Jiliang Software Co., Shanghai, China) software (Peng et al., 2010).

2.5. Tissue preparations and immunohistochemistry

Mice were subjected to deep anesthesia with 300 mg/kg i.p. chloral hydrate and treated with saline followed by a cold 4% paraformaldehyde during transcardiac perfusion. Brain tissues were then extracted and post-fixed in 4% paraformaldehyde overnight at 4 °C. After successively infiltrated with in 0.1 M PBS containing 20% and 30% sucrose overnight, coronal sections in 12 μm thicknesses were cut and stored at −20 °C until use. For BrdU immunohistochemistry, brain tissue sections were incubated in HCl (1 N) for 40 min at 45 °C to break open the DNA structure of the labeled cells, as previously described (Fournier et al., 2012; Wojtowicz and Kee, 2006). Immediately after the acid wash, borate buffer (0.1 M) was added to the cells. All sections were then incubated in a blocking solution for 1 h prior incubation with 1:100 rat-anti-BrdU (Abcam, USA) diluted in PBS at 4 °C for 48 h. Following incubation with the primary antibody, these sections were treated with 1:100 biotinylated goat–anti-rat (Vector, USA) at room temperature for 2 h followed by treatment with 1:1000 rhodamine–avidin D anti-mouse IgG (Vector, USA) at room temperature for 2 h. For Ki67 (the marker of cell proliferation) and DCX (donblecortin, the marker of developing, immature neurons) staining, sections were first treated with 1:1000 anti-rabbit Ki67 (Abcam, USA) and 1:2000 anti-rabbit DCX (Abcam, USA) antibodies at 4 °C overnight. After washing in PBS, sections were then incubated in 1:500 Alexa Fluor 488-conjugated donkey anti-rabbit (Invitrogen, USA) and 1:500 Alexa Fluor 594-conjugated goat anti-rabbit (Invitrogen, USA) secondary antibodies at room temperature for 4 h. For double immunostaining, sections were incubated with rat anti-BrdU first, as described previously. After treatment with a biotinylated goat–anti-rat and Rhodamine–avidin D, these sections were washed in PBS and treated with 1:100 mouse anti-NeuN (Chemicon, USA) at 4 °C overnight followed by treatment with 1:500 Alexa Fluor488-conjugated anti-rat IgG (Invitrogen, USA) at room temperature for 4 h. Finally, sections were incubated with Hochest 33342 for 10 min at room temperature to stain cell nuclei.

2.6. Cell culture and drug administration

Embryonic brains between E14.5 and E16.5 were dissected under a stereomicroscope, and single cell suspensions from the hippocampus were obtained by mechanical dissociation. Cell suspensions were primarily plated at a density of 5 × 10^5 cells/ml in 25 cm^2 Corning (USA) cell culture flasks using serum free Dulbecco's modified Eagle's medium (DMEM)/F12 medium containing 20 ng/ml bFGF (human recombinant, Peprotech, 100-18B, USA), 20 ng/ml EGF (rat recombinant, Peprotech, 400-25, USA), B-27 and N-2 supplement (Gibco, USA), and penicillin and streptomycin. The resultant neurospheres were harvested and mechanically dissociated to produce a single cell suspension for replating every 6–7 d. All experiments were performed during the second or third passage, after which single cells were resuspended. Cells were seeded onto plates or cover clips for 1 h, and rhTrx-1 was added to the culture medium at variant concentrations. The ERK signaling pathway was inhibited by adding 4 μM of U0126 (Sigma-Aldrich, USA) to the medium 0.5 h prior to rhTrx-1 administration.

2.7. Immunocytochemistry

To verify the identity of NSCs, neurospheres or single cells were collected and fixed in 4% paraformaldehyde. Frozen sections of the neurospheres and single cells on the cover slips were incubated with a mouse anti-nestin antibody (1:500, Abcam, Hong Kong) overnight at 4 °C. Immunolabeling was visualized by an anti-mouse Alexa Fluor 594-conjugated secondary antibody (1:500, Invitrogen).

Proliferation assay was performed after NSCs were incubated with rhTrx-1 for 2 d. rhTrx-1-treated neurospheres were labeled with 10 μM BrdU for 2 h and then dissociated into single cells and plated onto poly-L-lysine coated cover clips at a concentration of 2 × 10^4 cells per well in 24-well plates. After a 6 h attachment period, cells were fixed in 4% paraformaldehyde for 45 min. The fixative was then removed, and cells were incubated in HCl (1 N) for 30 min at 37 °C to break open the DNA structure of the labeled cells. Immediately after acid washing, cells were incubated with borate

buffer (0.1 M) for 10 min and processed for BrdU staining. In Ki67 staining experiments, cells were plated onto cover slips at a density of 2×10^4 cells per well in 24-well plates and treated with rhTrx-1. For immunostaining, cells were incubated at 4 °C overnight in PBS supplemented with 1% bovine serum albumin (BSA) and 0.3% Triton-X100 and either rat-anti-BrdU (1:100, Abcam, USA) or rabbit anti-Ki67 antibody (1:1000, Abcam, USA). Following incubation with rat anti-BrdU, cells were treated with 1:100 biotinylated goat anti-rat IgG (Vector, USA) at room temperature for 2 h followed by treatment with 1:1000 rhodamine–avidin D anti-mouse IgG (Vector, USA) at room temperature for 2 h. Following incubation with Ki67, cells were incubated with a fluorophore-conjugated secondary antibody (Alexa Fluor 488, 1:500, Invitrogen, USA) for 2 h at room temperature. Cells were further counter-stained using 50 μg/ml propidium iodide (PI, Sigma–Aldrich, USA) or DAPI for nuclei staining. BrdU-labeled and Ki67-positive cells were counted and normalized to the total cell count.

NSCs were phenotyped 7 days after rhTrx-1 treatment by protein marker expression. Cells were seeded on poly-D-lysine-coated cover clips at a density of 3×10^4 cells/well in DMEM/F12 medium containing 4% fetal bovine serum (Sigma–Aldrich, USA) and treated with rhTrx-1 for 7 d. After fixation, cells were incubated at 4 °C overnight with the primary antibodies composed of 1:500 mouse anti-Tuj1 (the marker of differentiated neurons; Sigma–Aldrich, USA) and 1:2000 rabbit anti-GFAP (the marker of differentiated astrocytes; Millipore, USA) diluted in blocking reagent and then incubated with 1:500 secondary antibodies (Alexa Fluor 488 or Alexa Fluor 594, Invitrogen, USA) for 2 h at room temperature. Finally, cells were incubated with DAPI to stain the nuclei.

2.8. Western blot

Cells were collected and lysed with SDS-PAGE sample buffer composed of 62.5 mM Tris–HCl, 2% w/v SDS, 10% glycerol, 50 mM DTT, and 0.1% w/v bromphenol blue. Insoluble materials were separated by centrifugation at 12,000 g for 10 min, and the supernatant was heated at 100 °C for 10 min and then cooled on ice for 30 min. Electrophoresis was conducted by SDS-PAGE by using 10% polyacrylamide in accordance with routine protocols. Then the proteins in PAGE were transferred onto nitrocellulose membranes and blocked in blocking solution containing 5% defatted milk powder, 0.1% Tween-20 in TBS for 1 h at room temperature with gentle shaking. After being washed in TBS 3 times for 8 min each, the following primary antibodies were used for incubation overnight at 4 °C: 1:2500 rabbit anti-pERK1/2 (Cell Signaling, USA), 1:2500 rabbit anti-ERK1/2 (Cell Signaling, USA), 1:1000 mouse anti-pAkt (Cell Signaling, USA), 1:1000 total Akt (Cell Signaling, USA), 1:1000 rabbit anti-Tuj1 (Sigma–Aldrich, USA), 1:5000 rabbit anti-GFAP (Millipore, USA), and 1:10000 rabbit anti-GAPDH antibody (Sigma–Aldrich, USA) as a loading control. All membranes were then washed 3 times in TBS and incubated with peroxidase-conjugated goat anti-rabbit IgG or peroxidase-conjugated goat anti-mouse IgG in TBST for 1 h. Immunoreactive bands were detected using enhanced chemiluminescence (ECL; Amersham, UK)

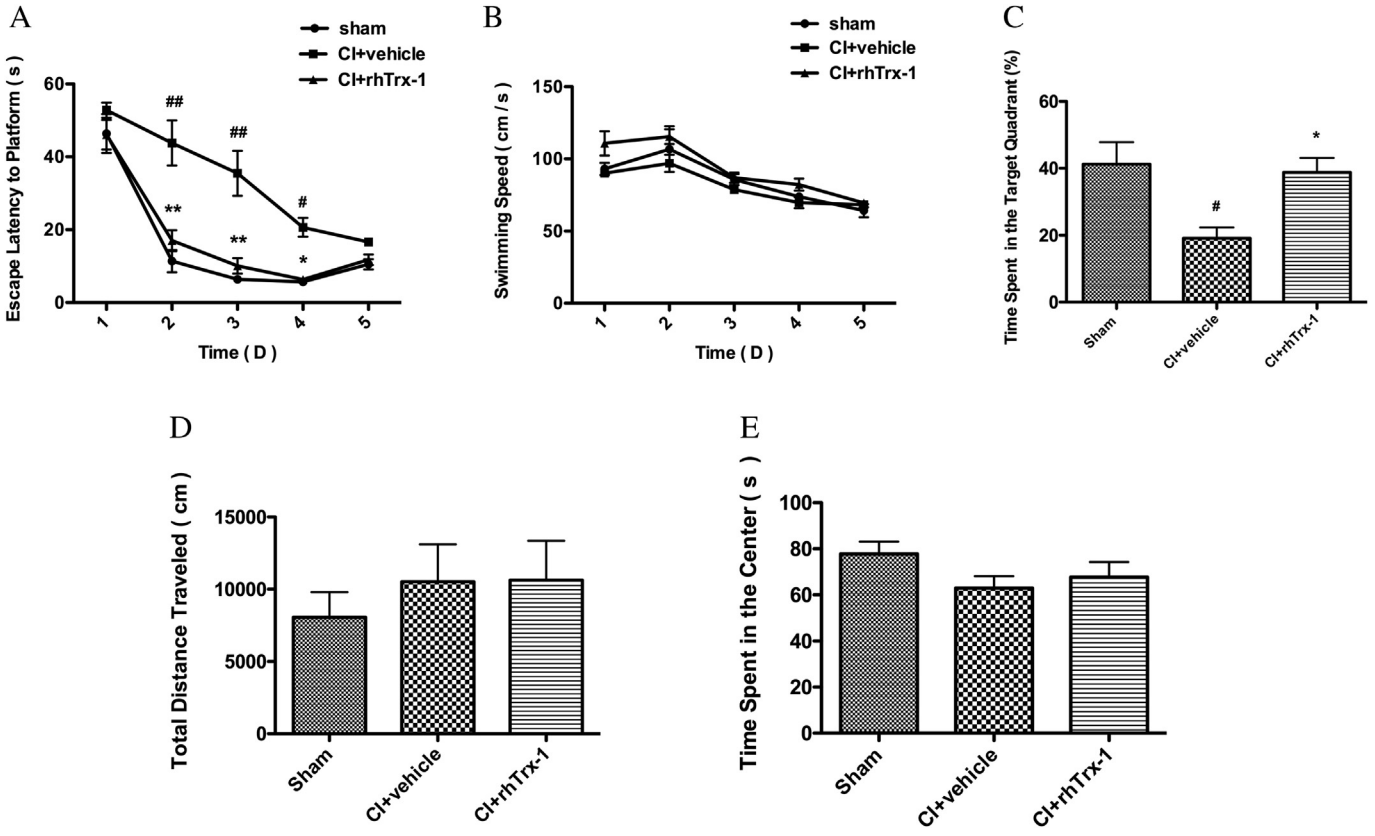

Fig. 2. rhTrx-1 facilitated ischemia-induced spatial learning and memory deficits. (A) Escape latency to find the hidden platform in MWM testing. (B). No difference in swimming speed was observed between the three groups. (C). Percentage of time spent in the target quadrant in the probe trial. (D) Total distance traveled in the open field test. (E) Time spent in the center in the open field test. Mice were subjected to a sham operation (Sham), BCCAO for 20 min with vehicle administration (CI + Vehicle) and BCCAO for 20 min with rhTrx-1 administration (CI + rhTrx-1). The MWM test and open field test were performed 30 days after reperfusion. Data were analyzed by two-way ANOVA with repeated measurement, followed by a Tukey post-hoc test and expressed as means ± S.E.M. from 8 independent animals ($n = 8$). $^{\#}P < 0.05$, $^{\#\#}P < 0.01$ vs sham-operated group; $^{*}P < 0.05$, $^{**}P < 0.01$ vs CI + Vehicle group.

and quantified with Bio-Rad Quantity One (Hercules, CA, USA) software.

2.9. Statistical analysis and quantification

All preparations were analyzed under an FV-1000 laser scanning confocal microscope (Olympus, USA) and positive cells were measured using Image-Pro Plus version 6.0 (Media Cybernetics, USA) software. An experimenter blinded to group assignments counted all proliferating precursors ($BrdU^+$ and $Ki67^+$ cells) in the entire granule cell layer (GCL). For quantitation of $BrdU^+$- and $Ki67^+$-labeled cells in the dentate gyrus of each mouse brain, every sixth section of the dorsal hippocampus was processed. Results were expressed as the number of labeled cells. Cells in the GCL and adjacent subgranular zone (SGZ) were defined as two-cell body-wide zones of the hilus along the base of the GCL and were counted,

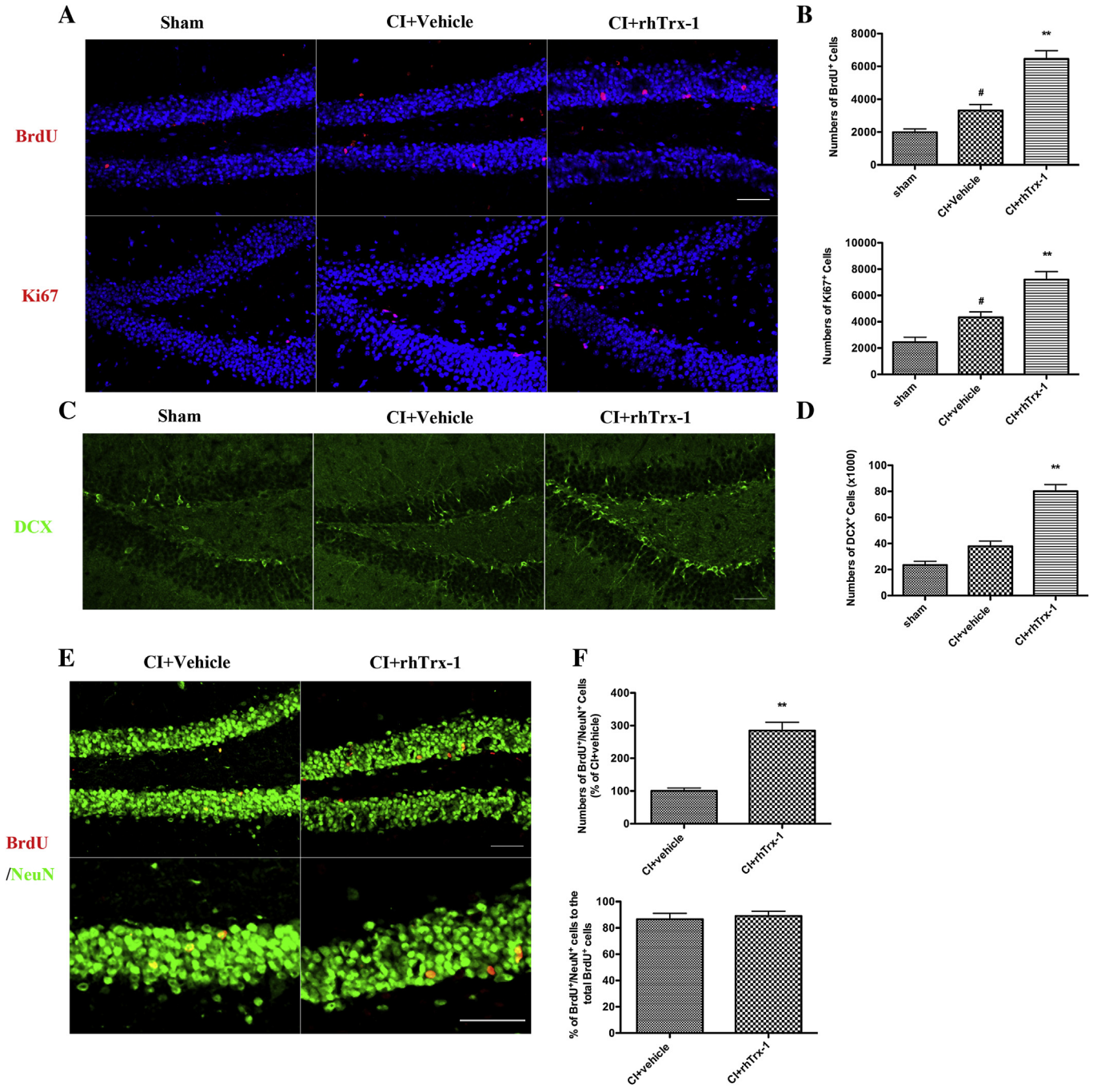

Fig. 3. rhTrx-1 promoted neurogenesis in the hippocampal dentate gyrus. (A, B) Microphotographs and histograms showing BrdU (*red*) and Ki67 (*red*) positive cells in the dentate gyrus of each group 14 days after reperfusion. (C, D) Microphotographs and histograms showing DCX (*green*) positive cells in the dentate gyrus of each group 14 days after reperfusion. (E) Representative confocal microscopic images showing BrdU (*red*) and NeuN (*green*) double-stained cells 30 days after reperfusion. (F) Histograms showing the number of $BrdU^+/NeuN^+$ cells (*upper*) and the percentage of $BrdU^+/NeuN^+$ cells to the total $BrdU^+$ cells (*lower*). Scale bar: 50 μm. Data were analyzed by one-way ANOVA, followed by Tukey post-hoc test and expressed as means ± S.E.M. from six independent animals ($n = 6$). $^{\#}P < 0.05$, $^{\#\#}P < 0.01$ vs sham-operated group; $^{*}P < 0.05$, $^{**}P < 0.01$ vs CI + Vehicle group.

according to previous methods (Brown et al., 2003; Maysami et al., 2008). Total numbers of DCX-labeled cells in the DG were counted under light microscopy for each mouse. DCX^+ neurons and granule cells were counted throughout the section thickness, excluding cells in the uppermost focal plane (Fuss et al., 2010; Naylor et al., 2008). For quantification of double-labeled cells, the percentage number of new neurons (60 $BrdU^+$ cells per mouse) was assessed using confocal microscopy. The percentages of $BrdU^+/NeuN^+$ cells to the absolute number of $BrdU^+$ cells was calculated to provide a ratio of newly generated neurons (Jiang et al., 2005).

In the *in vitro* experiment, BrdU-, Ki67-, Tuj1-, and GFAP-labeled cells were counted. Results were expressed as a percentage to the total cells indicated by PI or DAPI staining. At least 3–5 independent experiments were performed for each assay.

All data were analyzed using GraphPad Prism (GraphPad, USA) software. Histological data as well as relevant data from *in vivo* and *in vitro* assays were analyzed by one-way ANOVA followed by Tukey post-hoc testing in order to investigate the differences between sham, CI + Vehicle, and CI + rhTrx-1 groups at corresponding time intervals. Behavioral testing data were analyzed by repeated-measure two-way ANOVA, and probe trail testing data were analyzed by one-way ANOVA followed by Tukey post-hoc testing. Results were presented as mean ± standard error of the mean (SEM). A *P*-value of less than 0.05 was considered significant ($P < 0.05$), and a *P*-value of less than 0.01 was considered highly significant ($P < 0.01$).

3. Results

3.1. rhTrx-1 ameliorated spatial learning and memory deficits induced by ischemia

In the Morris Water Maze test, long latent period were initially required to find the platform for all mouse subjects, though this time decreased with progressive trial number. Sham-operated and CI + rhTrx-1 groups showed no significant differences in task-learning abilities and similar latency reduction rates ($P > 0.05$). Mice in the CI + Vehicle group, however, required increased time to locate the submerged platform compared with times in the rhTrx-1 and sham groups for each training day in MWM testing. Consistent with these findings, two-way ANOVA indicated that group and day exerted significant effects on escape latency. At test day 1, CI + Vehicle mice required longer times to find the platform relative to the CI + rhTrx-1 group; however, no statistical difference was observed ($P > 0.05$). By days 2–4, the time required to find the platform in the CI + Vehicle group was notably longer than those in both the sham-operated and CI + rhTrx-1 groups (Fig. 2A, $P < 0.01$ at day 1 and 3; $P < 0.05$ at day 4) groups. Swimming speed during the test was also evaluated and analyzed by two-way ANOVA, demonstrating no group or day effects on swimming speed (Fig. 2B, $P > 0.05$). In the probe trial test, both sham-operated and CI + rhTrx-1 group mice appeared to have learned the task, demonstrating superior ability to remember the platform location

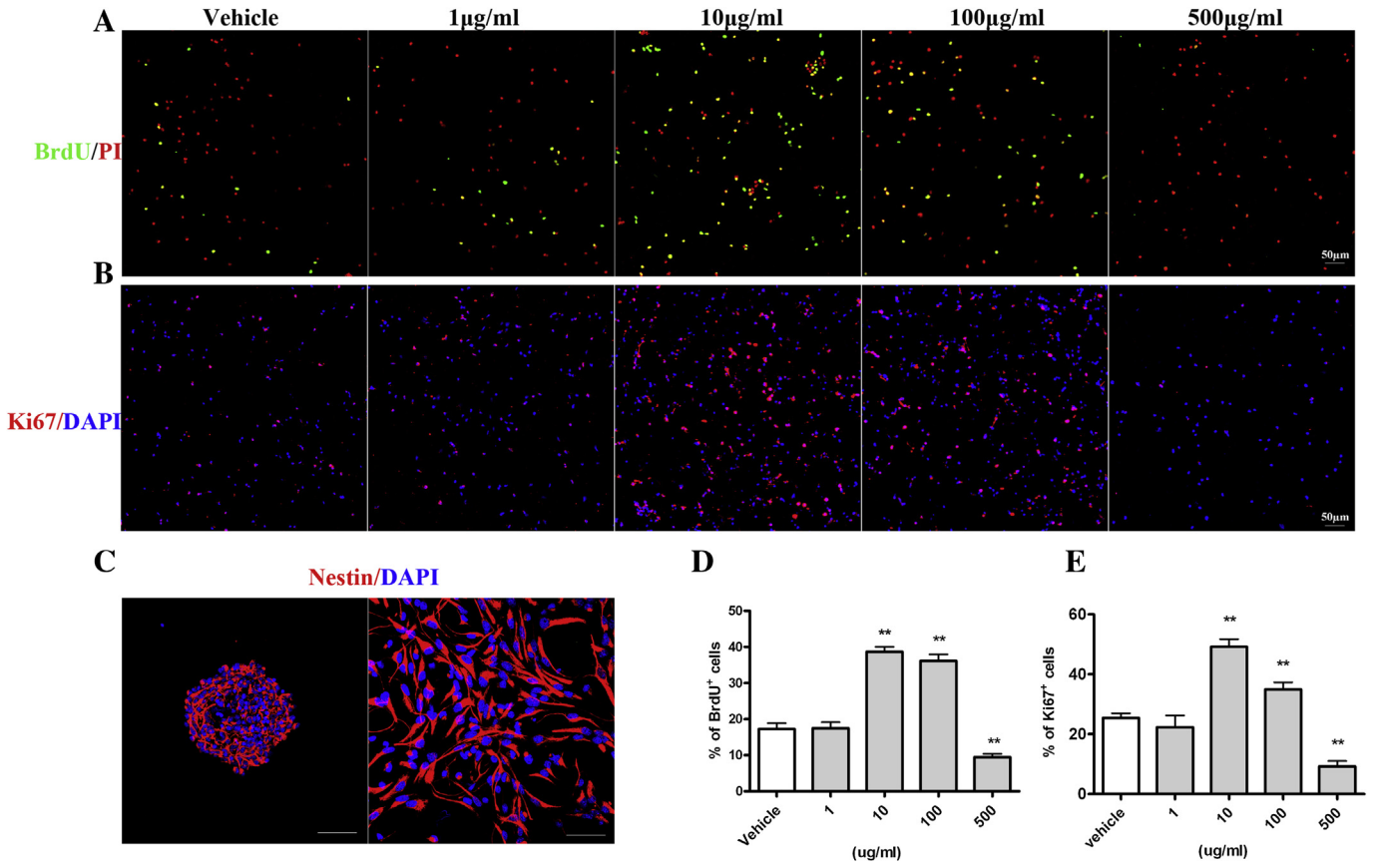

Fig. 4. rhTrx-1 promoted proliferation of cultured NSCs in a dose dependent manner. (A, B) Immunofluorescence images of BrdU (*green*)/PI (*red*) and Ki67 (*red*)/DAPI (*blue*) stained NSCs after incubation with vehicle and rhTrx-1 of variant concentrations for 48 h. (C) Immunofluorescence image of single neural cells and a neurosphere that were fixed and stained with nestin (*red*) and then counterstained with DAPI (*blue*) as the nuclear marker. (D, E) Quantitation of BrdU and Ki67 positive cells showing a significant increase in the number of dividing cells in rhTrx-1 groups relative to the vehicle group. Scale bar: 50 μm. Data were analyzed by one-way ANOVA, followed by Tukey post-hoc test and expressed as mean ± S.E.M. from 5 wells per treatment condition. $^*P < 0.05$, $^{**}P < 0.01$ vs Vehicle group.

compares to vehicle-treated mice. This effect was evidenced by significantly longer periods of time spent in the target quadrant in the sham-operated and CI + rhTrx-1 groups compared to the CI + Vehicle group (Fig. 2C, $P < 0.05$).

To assess whether reduced activity levels could have contributed to impairments in MWM performance following ischemia, experimental mice were tested for open-field activity. In the open field test, no significant difference in horizontal distance of travel in

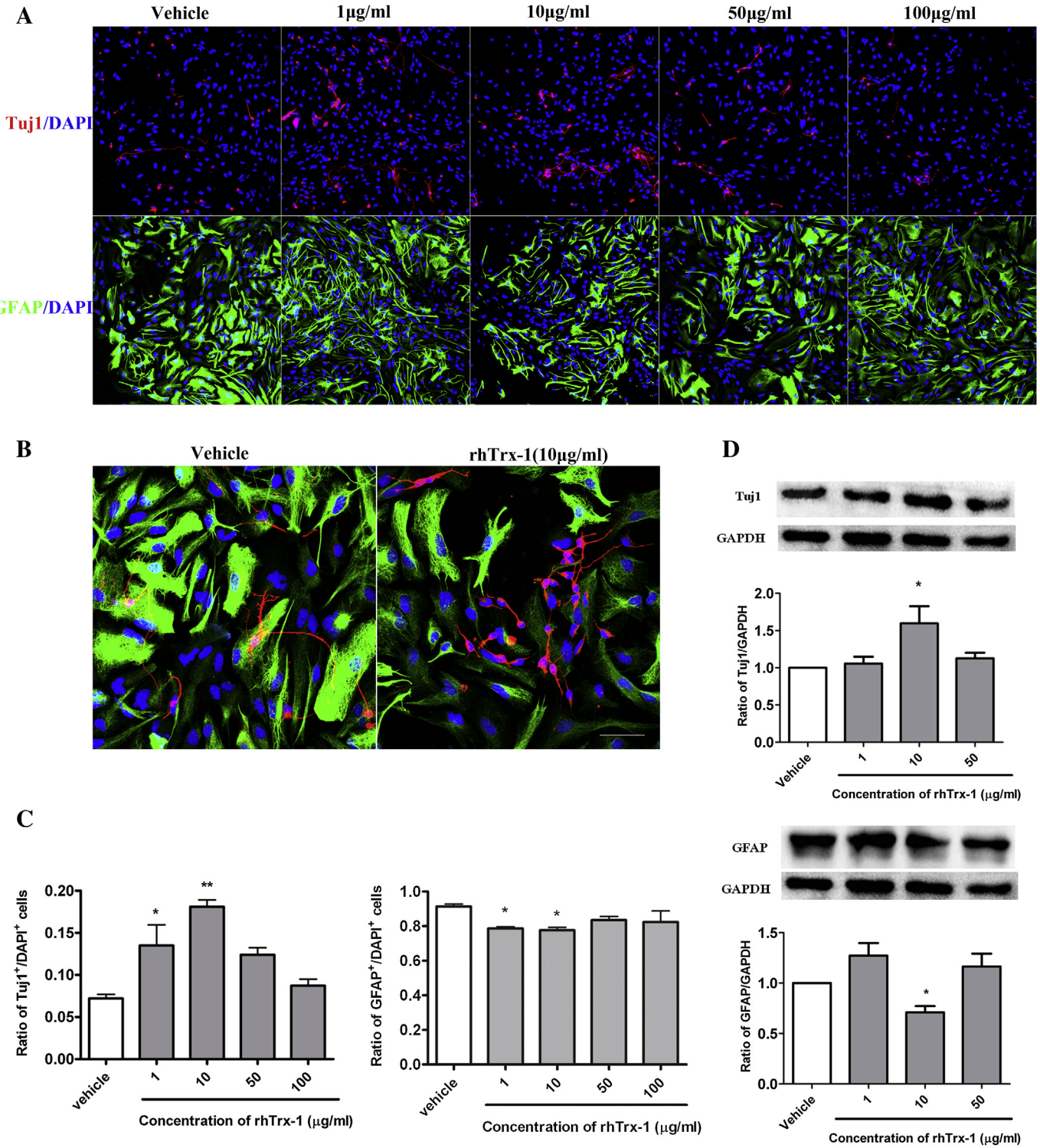

Fig. 5. rhTrx-1 promoted cultured NSC differentiation into neurons. (A) Immunofluorescence images of Tuj1 (*red*), GFAP (*green*), and DAPI (*blue*) stained NSCs after incubation with vehicle or rhTrx-1 of variant concentrations for 7 days. (B) High magnification of the images from vehicle and rhTrx-1 (10 μg/ml) groups. (C) Histograms of the percentage of Tuj positive cells to the total DAPI positive cells (*left*) and the percentage of GFAP positive cells to the total DAPI positive cells (*right*). (D) Expression of Tuj1 and GFAP in each group determined by Western blot. Representative bands and densitometric analysis of Tuj1 (*upper*) and GFAP (*lower*) with GAPDH as the loading control. Scale bar: 50 μm. Data were analyzed by one-way ANOVA, followed by Tukey post-hoc test and expressed as mean ± S.E.M. from 5 wells per treatment condition. $^{*}P < 0.05$, $^{**}P < 0.01$ vs Vehicle group.

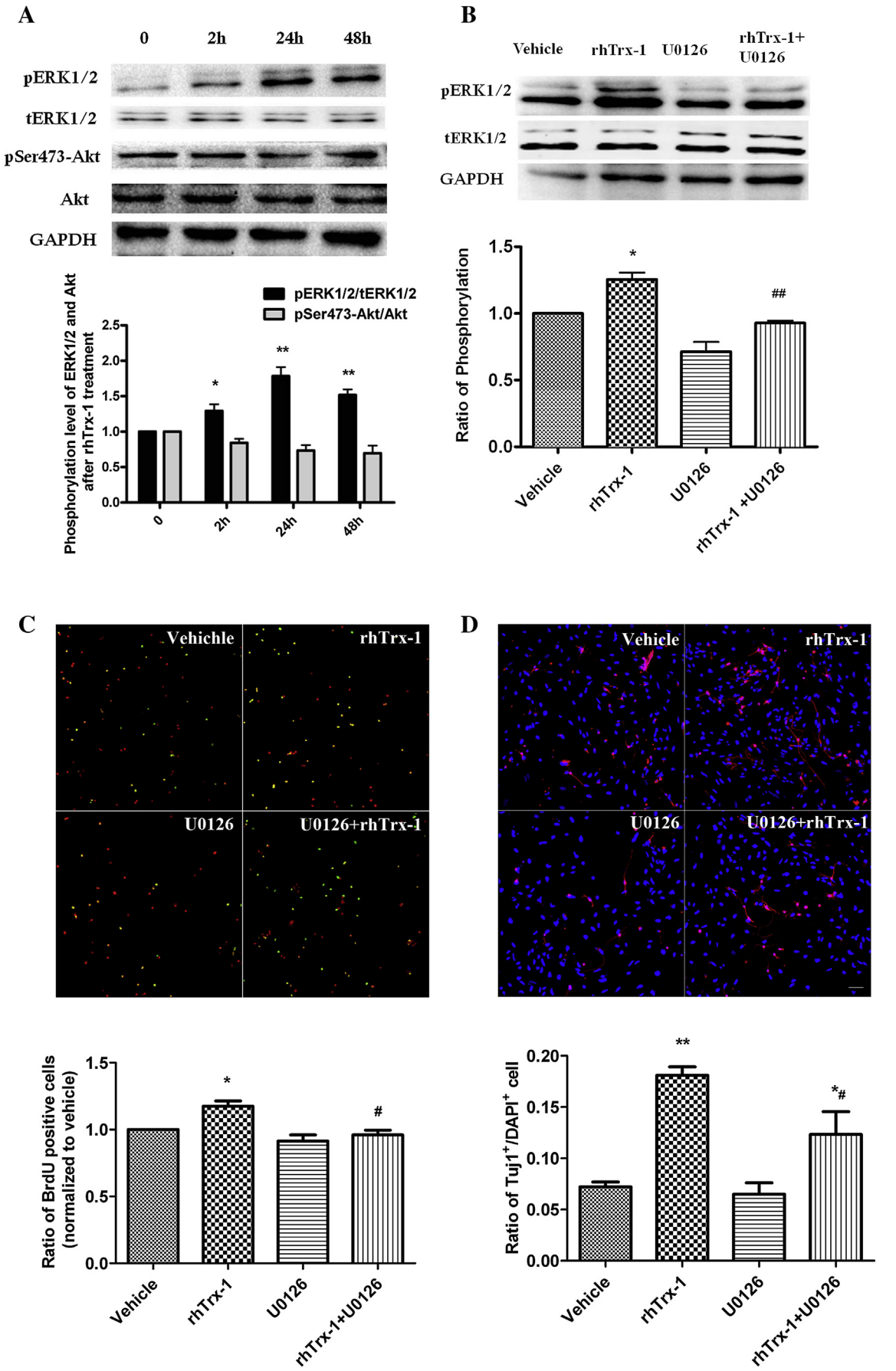
A
0
2h
24h
48h
pERK1/2
tERK1/2
pSer473-Akt
Akt
GAPDH
pERK1/2/tERK1/2
pSer473-Akt/Akt
Phosphorylation level of ERK1/2 and Akt after rhTrx-1 treatment
B
Vehicle
rhTrx-1
U0126
rhTrx-1+ U0126
pERK1/2
tERK1/2
GAPDH
Ratio of Phosphorylation
Vehicle
rhTrx-1
U0126
rhTrx-1 +U0126
C
Vehichle
rhTrx-1
U0126
U0126+rhTrx-1
Ratio of BrdU positive cells (normalized to vehicle)
D
Vehicle
rhTrx-1
U0126
U0126+rhTrx-1
Ratio of Tuj1+/DAPI+ cell

the chamber was observed among the three groups (Fig. 2D, $P > 0.05$). In addition, the number of entries to the central zone of the open field was recorded in order to assess mouse anxiety level. No significant difference was observed in center zone time for any group (Fig. 2E, $P > 0.05$).

3.2. rhTrx-1 promoted ischemia-induced neurogenesis in DG

To investigate the effect of rhTrx-1 on proliferation of the neural stem cells following forebrain ischemia, the cells incorporated with BrdU and those stained with Ki67 in the DG were counted (Fig. 3A). At post-ischemic day 14, the number of $BrdU^+$ cells increased approximately 1.5-fold in the CI + Vehicle group compared with the sham-operated group (Fig. 3B; $P < 0.05$). In addition, administration of rhTrx-1 significantly increased the number of $BrdU^+$ cells compared with the CI + Vehicle group ($P < 0.01$). Similarly, the CI + Vehicle group showed increased numbers of $Ki67^+$ cells (Fig. 3B; $P < 0.05$) and this number reached approximately 2-fold in CI + rhTrx-1 group ($P < 0.01$). DCX expression was used to estimate cycling precursors of neuronal lineage as well as maturing young granule cells (Fuss et al., 2010) (Couillard-Despres et al., 2005). The CI + rhTrx-1 group demonstrated a significant increase in the number of DCX^+ cells in the DG (Fig. 3C, D; $P < 0.01$).

To estimate the effect of rhTrx-1 on the differentiation of NSCs, double labeling of BrdU and NeuN was performed 30 days after ischemia (Fig. 3E). The number of $BrdU^+$ cells in the CI + rhTrx-1 group was much larger than that observed in the CI + Vehicle group (Fig. 3F; $P < 0.01$), indicating the survival of the majority of rhTrx-1-induced new neural cells. Although many $BrdU^+$ cells were still found in the DG, immunofluorescence staining revealed that the proportion of $BrdU^+/NeuN^+$ double-labeled cells to total $BrdU^+$ cells in both the CI + rhTrx-1 and CI + Vehicle groups were similar ($P > 0.05$).

3.3. rhTrx-1 enhanced proliferation of cultured NSCs

To investigate the direct effects of rhTrx-1 on NSCs and to study the underlying mechanism, *in vitro* study was also conducted. As shown in Fig. 4C, neurospheres and single cells expressed nestin, a marker of NSCs. After treatment with different concentrations of rhTrx-1 for 48 h, the percentage of BrdU labeled cells was higher in 10 and 100 μg/ml rhTrx-1 treatments compared to the vehicle group, while less BrdU positive cells were seen in the 500 μg/ml treated group (Fig. 4A, D; $P < 0.01$). The results of Ki67 staining also revealed that rhTrx-1 promoted proliferation of NSCs at concentrations of 10 and 100 μg/ml, but inhibited proliferation at 500 μg/ml (Fig. 4B, E; $P < 0.01$).

3.4. rhTrx-1 promoted NSCs differentiating into neurons

After treatment with rhTrx-1 for 7 days, expression of Tuj1 and GFAP were examined (Fig. 5A). Immunocytochemical results revealed that the ratio of differentiated neurons was higher in groups treated with both 1 μg/ml (13.51%) and 10 μg/ml (18.08%) rhTrx-1 compared with the vehicle group (7.21%) (Fig. 5C; $P < 0.05$ at 1 μg/ml, $P < 0.01$ at 10 μg/ml). Western blot analysis showed that Tuj1 expression of NSCs in the 10 μg/ml treatment group was increased approximately 1.5-fold compared to the vehicle group (Fig. 5D, $P < 0.05$). The ratio of GFAP positive cells and the expression of GFAP in NSCs were decreased when cells were incubated in 10 μg/ml of rhTrx-1 (Fig. 5C, D; $P < 0.05$).

3.5. Neurogenesis enhanced by rhTrx-1 was inhibited by U0126

Both MEK/ERK and PI3K/Akt signaling pathways have been implicated in the mechanism of proliferation and neurogenesis of NSCs. The activation of these pathways during rhTrx-1 treatment and subsequent induction of proliferation and neurogenesis were explored using a 10 μg/ml rhTrx-1 treatment to further study this mechanism. Expression of phosphorylated ERK1/2 began to increase at 2 h, maintain a high level to 48 h after rhTrx-1 administration (Fig. 6A; $P < 0.05$ at 2 h, $P < 0.01$ at 24 h and 48 h). The levels of phosphorylated Akt did not significantly change after NSCs incubation with rhTrx-1 ($P > 0.05$). Western blot analysis of the protein sample, extracted from NSCs cultured for 48 h in proliferation medium revealed that pretreatment with the inhibitor of ERK1/2 U0126 inhibited the elevation of the phosphorylated ERK1/2 induced by rhTrx-1 (Fig. 6B; $P < 0.01$). Furthermore, U0126 suppressed increases in the ratio of BrdU labeled cells in the rhTrx-1 treated group (Fig. 6C; $P < 0.05$). Also, co-administration with U0126 decreased the percentage of neuronal differentiation (Fig. 6D, $P < 0.05$) compared to levels observed in the rhTrx-1 group ($P < 0.01$).

4. Discussion

The prominent effects of rhTrx-1 treatment for improving spatial learning and memory impairments in adult mice subjected to global CI were demonstrated in the present study. Moreover, rhTrx-1 was demonstrated to promote neurogenesis in the DG, indicating that rhTrx-1 potentially plays a role in the induction of neurogenesis and the facilitation of cognitive recovery following ischemia of cerebral tissues in mice. The *in vitro* study of rhTrx-1 in mice further demonstrated that the treatment also has the ability to enhance NSC proliferation and differentiation to neural cells. Furthermore, the ERK signaling pathway participated in stimulated neurogenesis.

The hippocampus is associated with the processes of learning and memory in mammals (Auer et al., 1989; Squire, 1992). In previous studies, it has been reported that 20 min of BCCAO treatment can obliterate more than 50% of all hippocampal CA1 neurons (Zhang et al., 2010), contributing to significant learning impairments visualized in mice by MWM testing (Block, 1999; Raber et al., 2004). With rhTrx-1 treatment, functional impairments resulting from such ischemic periods were significantly improved at post-ischemic day 30, as demonstrated by both training and probe trail testing results in the current study. These results suggest that exogenous administration of rhTrx-1 may facilitate persistent cognitive recovery following CI. Notably, mice treated with rhTrx-1 displayed equivalent swimming abilities during MWM testing and equivalent locomotion activity during open-field testing compared to other groups. Therefore, the functional impairments in ischemic

Fig. 6. The neurogenesis enhanced by rhTrx-1 was inhibited by U0126 in cultured NSCs. (A) Western blot analysis of expression of phosphorylated ERK1/2 and Akt in NSCs treated with vehicle or rhTrx-1 (10 μg/ml) for 2, 24, and 48 h. (B) Western blot analysis of expression of phosphorylated ERK1/2 in cultured NSCs after 2 d incubation with rhTrx-1 or U0126. (C) Immunofluorescence images and histograms showing the percentage of BrdU (*green*) positive cells to the total PI (*red*) stained cells after 2 d incubation with rhTrx-1 or U0126. (D) Immunofluorescence images and percentage of Tuj1 (*red*) positive cells to all DAPI (*blue*) stained cells after 7d rhTrx-1 or U0126 incubation. Cells treated with DMSO (vehicle), DMSO plus rhTrx-1 (rhTrx-1), U0126 dissolved in DMSO (U0126), and U0126 plus rhTrx-1 (rhTrx-1+U0126), respectively, for 2 d or 7 d according to proliferation and differentiation analysis. Scale bar: 50 μm. Data were analyzed by one-way ANOVA, followed by Tukey post-hoc test and expressed as mean ± S.E.M. from 5 wells per treatment condition. $^*P < 0.05$, $^{**}P < 0.01$ vs Vehicle group; $^{\#}P < 0.05$, $^{\#\#}P < 0.01$ vs rhTrx-1 group.

animals during the MWM testing may be partially or completely caused by deficits in task learning. These tests do, however demonstrate that these deficits are not related to limitations of normal motor functions.

A considerable degree of neurogenesis from endogenous precursors has been reported to occur following CI in the adult mammalian brain, as documented in various rodent models (Jin et al., 2001; Kee et al., 2001; Liu et al., 1998). This observation suggests the possibility that neuronal cells genesis might provide an alternative mechanism for post-ischemic functional recovery (Arvidsson et al., 2002; Carmichael, 2006; Hermann and Chopp, 2012). Neurogenesis occurs in 2 sites in the brain of adult mammals, the SGZ and the subventricular zone (SVZ) of the lateral ventricle. These regions comprise the entire capacity of neurogenesis throughout an animal's life (Cameron and McKay, 2001; Kempermann et al., 2004). The survival rate of adult neural precursor cells in the ischemic brain, however, is very poor. In fact, only a small percentage of these cells successfully differentiate into new neurons (Zhang et al., 2004, 2011). Thus, numerous therapeutic intervention strategies have been designed with the goal of promoting endogenous neurogenesis and subsequent survival of implanted neural stem cells (Bartolini et al., 2011; Wei et al., 2012). The current results demonstrate that administration of rhTrx-1 exerted significant proliferative effects on hippocampal precursors. Combined with previous reports, these findings may indicate that the cellular mechanisms underlying the protective effects of rhTrx-1 may vary during different reperfusion stages following ischemia. In early stages following ischemia, rhTrx-1 may reduce apoptotic death, thus exerting neuronal protection (Ma et al., 2012). During late stages, rhTrx-1 may increase generation and survival of new neurons in the hippocampus. In the adult mouse hippocampus, newly generated neural cells are functionally integrated into the hippocampal circuitry by 4 weeks and display passive membrane properties, action potentials, and functional synaptic inputs similar to those found in mature dentate granule cells (van Praag et al., 2002). Considering these observations, functional recovery at 4 weeks after rhTrx-1 administration may be attributable to the neurogenesis promotion effects of rhTrx-1. The current histological and Western blot results also confirm that neural cell proliferation was markedly increased after administration of 10 μg/ml rhTrx-1. Similarly, differentiation of NSCs into neurons was also stimulated in cultured cells in the present study. However, we noticed that administration of much higher concentration of rhTrx-1 (500 μg/ml) showed an inhibiting action on the proliferation of cultured neural stem cells inversely, indicating a bell shape effect of rhTrx-1 on proliferation. Interestingly, it has been reported that the chemotactic effect of rhTrx-1 on human PMNs and T cells is also manifested as a typical bell-shaped dose–response curve (Bertini et al., 1999). Based on these data, it may be tentatively concluded that rhTrx-1 facilitates cell repair in hippocampus through stimulation of neurogenesis by endogenous progenitor cells, thus improving behavioral recovery. Although these results provide evidence supporting the hypothesis that neurogenesis contributes to the neuroprotective effects of rhTrx-1 following ischemic injury in brain tissues, the possibility that other potential effects of rhTrx-1 are also involved in the recovery of behavior cannot be excluded.

Both the MEK/ERK and PI3K/Akt signaling pathways participate in neurogenesis following cerebral ischemia (Kilic et al., 2006; Shioda et al., 2009). The ERK signaling cascade is reported to control the proliferation of multiple cell types, including neural stem/progenitor cells, especially in response to growth factor treatment (Li et al., 2001; Wang et al., 2009). The current study revealed that administration of rhTrx-1 increased the level of activated ERK1/2. These findings were confirmed by abolishment of rhTrx1-induced proliferation when the ERK signaling pathway was blocked by U0126, also dramatically reducing expression of the neuronal marker Tuj1. Although accumulating evidence supports the effect of the PI3K/Akt signaling pathway in cell cycle regulation (Liang and Slingerland, 2003), stem cell self-renewal, and neuronal cell number and composition (Easton et al., 2005; Tschopp et al., 2005), no significant changes in pAkt level were reported in mice treated with rhTrx-1. Cumulatively, these data suggest that the ERK signaling pathway is necessary for regulation of proliferation and differentiation in NSCs treated with rhTrx-1. The potential role of rhTrx-1 in the activation of the ERK signaling pathway, however, was not determined by this study. Recent evidence has demonstrated that vascular endothelial growth factor (VEGF) has a broad range of neurotropic and neuroprotective effects in the central nervous system (CNS) (Ruiz de Almodovar et al., 2009), where it stimulates self-renewal of both embryonic and adult NSCs through the MEK/ERK and PI3K/Akt signaling pathways (Fournier et al., 2012; Shen et al., 2004). Conversely, Trx1 is able to regulate VEGF levels in both embryonic and adult neural stem cells under either normoxic or hypoxic conditions, thus promoting angiogenesis by acting on hypoxia inducible factor 1α (HIF-1α) (Welsh et al., 2002). Therefore, rhTrx-1 is possibly both a neurogenic and angiogenic factor, promoting neurogenesis through the ERK signaling pathway in the CNS.

Neural stem cells play a pivotal role in self-renewal, potentially differentiating into various different cytotypes (Doe, 2008; Shimazaki and Okano, 2008). Neurogenesis in the SGZ has been shown to be related to exercise, spatial learning, and memory (Gould et al., 1999; van Praag et al., 1999). Moreover, active neurogenesis is crucial for injury repair to morphological changes in the hippocampus caused by neuron loss associated with either ischemia or neurodegenerative diseases, such as Alzheimer's disease, rheumatoid arthritis and stroke, or trauma (Ramirez-Ruiz et al., 2005; Wang et al., 2001). Therefore, development of new drugs and treatments to promote neurogenesis may enable replenishment of lost neurons, providing a promising strategy for treatment of these neurodegenerative diseases. In fact, several neuronal growth factors have been demonstrated to promote neurogenesis, as previously described. In addition, recent evidence has demonstrated the importance of the relationship between neural stem/progenitor cells and vasculature (Louissaint et al., 2002; Palmer et al., 2000; Shen et al., 2004). Cumulatively, these findings provide compelling evidence for the coordination of angiogenesis and neurogenesis in the CNS; however, clinical application remains limited by low bioavailability and the limited capacity of most drug therapies to cross the blood–brain barrier. Trx1 is a small redox protein present in many organisms, where it plays a role in important biological processes and endothelial cells angiogenesis. Moreover, Trx1 crosses the blood–brain barrier. Thus, rhTrx-1 exhibits favorable pharmacokinetics and a good safety profile for human applications, making it a prime candidate for angiogenesis and neurogenesis mediation in developing and adult brains.

The current study clearly demonstrates that rhTrx-1 is effective in promoting neurogenesis in the dentate gyrus and facilitating cognitive recovery following CI in adult mice. Additionally, the underlying mechanism of rhTrx-1 in neurogenesis was confirmed to be mediated by the ERK signaling pathway. These results suggest that rhTrx-1 may be a potential agent for the clinical treatment of ischemic injury in brain tissues.

Acknowledgments

We thank Dr. Bairen WANG (Professor, Institute of Neuroscience, Fourth Military Medical University, Xi'an Shaanxi, China) and Ming

Shi (Department of Neurology, Xijing Hospital, the Fourth Military Medical University, Xi'an Shaanxi, China) for reviewing the manuscript. This work was supported by the National Science Foundation for Distinguished the State Key Program of National Natural Science Foundation of China (Grant 30930091 to Lize Xiong), the National Natural Science Foundation of China (Grant 30972853 to HaiLong Dong and Grant 81100902 to Qianzi Yang).

References

Abraham, W.C., Logan, B., Greenwood, J.M., Dragunow, M., 2002. Induction and experience-dependent consolidation of stable long-term potentiation lasting months in the hippocampus. J. Neurosci. 22, 9626–9634.
Arvidsson, A., Collin, T., Kirik, D., Kokaia, Z., Lindvall, O., 2002. Neuronal replacement from endogenous precursors in the adult brain after stroke. Nat. Med. 8, 963–970.
Auer, R.N., Jensen, M.L., Whishaw, I.Q., 1989. Neurobehavioral deficit due to ischemic brain damage limited to half of the CA1 sector of the hippocampus. J. Neurosci. 9, 1641–1647.
Bartolini, A., Vigliani, M.C., Magrassi, L., Vercelli, A., Rossi, F., 2011. G-CSF administration to adult mice stimulates the proliferation of microglia but does not modify the outcome of ischemic injury. Neurobiol. Dis. 41, 640–649.
Bendel, O., Alkass, K., Bueters, T., von Euler, M., von Euler, G., 2005. Reproducible loss of CA1 neurons following carotid artery occlusion combined with halothane-induced hypotension. Brain Res. 1033, 135–142.
Bernabeu, R., Sharp, F.R., 2000. NMDA and AMPA/kainate glutamate receptors modulate dentate neurogenesis and CA3 synapsin-I in normal and ischemic hippocampus. J. Cereb. Blood Flow Metab. 20, 1669–1680.
Bertini, R., Howard, O.M., Dong, H.F., Oppenheim, J.J., Bizzarri, C., Sergi, R., Caselli, G., Pagliei, S., Romines, B., Wilshire, J.A., Mengozzi, M., Nakamura, H., Yodoi, J., Pekkari, K., Gurunath, R., Holmgren, A., Herzenberg, L.A., Herzenberg, L.A., Ghezzi, P., 1999. Thioredoxin, a redox enzyme released in infection and inflammation, is a unique chemoattractant for neutrophils, monocytes, and T cells. J. Exp. Med. 11, 1783–1789.
Block, F., 1999. Global ischemia and behavioural deficits. Prog. Neurobiol. 58, 279–295.
Brown, J., Cooper-Kuhn, C.M., Kempermann, G., Van Praag, H., Winkler, J., Gage, F.H., Kuhn, H.G., 2003. Enriched environment and physical activity stimulate hippocampal but not olfactory bulb neurogenesis. Eur. J. Neurosci. 17, 2042–2046.
Cameron, H.A., McKay, R.D., 2001. Adult neurogenesis produces a large pool of new granule cells in the dentate gyrus. J. Comp. Neurol. 435, 406–417.
Carmichael, S.T., 2006. Cellular and molecular mechanisms of neural repair after stroke: making waves. Ann. Neurol. 59, 735–742.
Chen, G., Chen, K.S., Knox, J., Inglis, J., Bernard, A., Martin, S.J., Justice, A., McConlogue, L., Games, D., Freedman, S.B., Morris, R.G., 2000. A learning deficit related to age and beta-amyloid plaques in a mouse model of Alzheimer's disease. Nature 408, 975–979.
Couillard-Despres, S., Winner, B., Schaubeck, S., Aigner, R., Vroemen, M., Weidner, N., Bogdahn, U., Winkler, J., Kuhn, H.G., Aigner, L., 2005. Doublecortin expression levels in adult brain reflect neurogenesis. Eur. J. Neurosci. 21, 1–14.
Deng, W., Aimone, J.B., Gage, F.H., 2010. New neurons and new memories: how does adult hippocampal neurogenesis affect learning and memory? Nat. Rev. Neurosci. 11, 339–350.
Doe, C.Q., 2008. Neural stem cells: balancing self-renewal with differentiation. Development 135, 1575–1587.
Dunn, L.L., Buckle, A.M., Cooke, J.P., Ng, M.K., 2010. The emerging role of the thioredoxin system in angiogenesis. Arterioscler Thromb. Vasc. Biol. 30, 2089–2098.
Easton, R.M., Cho, H., Roovers, K., Shineman, D.W., Mizrahi, M., Forman, M.S., Lee, V.M., Szabolcs, M., de Jong, R., Oltersdorf, T., Ludwig, T., Efstratiadis, A., Birnbaum, M.J., 2005. Role for Akt3/protein kinase Bgamma in attainment of normal brain size. Mol. Cell. Biol. 25, 1869–1878.
Fournier, N.M., Lee, B., Banasr, M., Elsayed, M., Duman, R.S., 2012. Vascular endothelial growth factor regulates adult hippocampal cell proliferation through MEK/ERK- and PI3K/Akt-dependent signaling. Neuropharmacology 63, 642–652.
Fuss, J., Ben Abdallah, N.M., Vogt, M.A., Touma, C., Pacifici, P.G., Palme, R., Witzemann, V., Hellweg, R., Gass, P., 2010. Voluntary exercise induces anxiety-like behavior in adult C57BL/6J mice correlating with hippocampal neurogenesis. Hippocampus 20, 364–376.
Gould, E., Beylin, A., Tanapat, P., Reeves, A., Shors, T.J., 1999. Learning enhances adult neurogenesis in the hippocampal formation. Nat. Neurosci. 2, 260–265.
Hartman, R.E., Lee, J.M., Zipfel, G.J., Wozniak, D.F., 2005. Characterizing learning deficits and hippocampal neuron loss following transient global cerebral ischemia in rats. Brain Res. 1043, 48–56.
Hattori, I., Takagi, Y., Nakamura, H., Nozaki, K., Bai, J., Kondo, N., Sugino, T., 2004. Intravenous administration of thioredoxin decreases brain damage following transient focal cerebral ischemia in mice. Antioxid. Redox Signal. 6 (1), 81–87.
Hermann, D.M., Chopp, M., 2012. Promoting brain remodelling and plasticity for stroke recovery: therapeutic promise and potential pitfalls of clinical translation. Lancet Neurol. 11, 369–380.
Homi, H.M., Mixco, J.M., Sheng, H., Grocott, H.P., Pearlstein, R.D., Warner, D.S., 2003. Severe hypotension is not essential for isoflurane neuroprotection against forebrain ischemia in mice. Anesthesiology 99, 1145–1151.
Jiang, W., Zhang, Y., Xiao, L., Van Cleemput, J., Ji, S.P., Bai, G., Zhang, X., 2005. Cannabinoids promote embryonic and adult hippocampus neurogenesis and produce anxiolytic- and antidepressant-like effects. J. Clin. Invest. 115, 3104–3116.
Jin, K., Minami, M., Lan, J.Q., Mao, X.O., Batteur, S., Simon, R.P., Greenberg, D.A., 2001. Neurogenesis in dentate subgranular zone and rostral subventricular zone after focal cerebral ischemia in the rat. Proc. Natl. Acad. Sci. U. S. A. 98, 4710–4715.
Kee, N.J., Preston, E., Wojtowicz, J.M., 2001. Enhanced neurogenesis after transient global ischemia in the dentate gyrus of the rat. Exp. Brain Res. 136, 313–320.
Kempermann, G., Jessberger, S., Steiner, B., Kronenberg, G., 2004. Milestones of neuronal development in the adult hippocampus. Trends Neurosci. 27, 447–452.
Kilic, U., Kilic, E., Jarve, A., Guo, Z., Spudich, A., Bieber, K., Barzena, U., Bassetti, C.L., Marti, H.H., Hermann, D.M., 2006. Human vascular endothelial growth factor protects axotomized retinal ganglion cells in vivo by activating ERK-1/2 and Akt pathways. J. Neurosci. 26, 12439–12446.
Lai, M., Horsburgh, K., Bae, S.E., Carter, R.N., Stenvers, D.J., Fowler, J.H., Yau, J.L., Gomez-Sanchez, C.E., Holmes, M.C., Kenyon, C.J., Seckl, J.R., Macleod, M.R., 2007. Forebrain mineralocorticoid receptor overexpression enhances memory, reduces anxiety and attenuates neuronal loss in cerebral ischaemia. Eur. J. Neurosci. 25, 1832–1842.
Li, B.S., Ma, W., Zhang, L., Barker, J.L., Stenger, D.A., Pant, H.C., 2001. Activation of phosphatidylinositol-3 kinase (PI-3K) and extracellular regulated kinases (Erk1/2) is involved in muscarinic receptor-mediated DNA synthesis in neural progenitor cells. J. Neurosci. 21, 1569–1579.
Liang, J., Slingerland, J.M., 2003. Multiple roles of the PI3K/PKB (Akt) pathway in cell cycle progression. Cell Cycle 2, 339–345.
Lichtenwalner, R.J., Parent, J.M., 2006. Adult neurogenesis and the ischemic forebrain. J. Cereb. Blood Flow Metab. 26, 1–20.
Liu, J., Solway, K., Messing, R.O., Sharp, F.R., 1998. Increased neurogenesis in the dentate gyrus after transient global ischemia in gerbils. J. Neurosci. 18, 7768–7778.
Louissaint Jr., A., Rao, S., Leventhal, C., Goldman, S.A., 2002. Coordinated interaction of neurogenesis and angiogenesis in the adult songbird brain. Neuron 34, 945–960.
Ma, Y.H., Su, N., Chao, X.D., Zhang, Y.Q., Zhang, L., Han, F., Luo, P., Fei, Z., Qu, Y., 2012. Thioredoxin-1 attenuates post-ischemic neuronal apoptosis via reducing oxidative/nitrative stress. Neurochem. Int. 60, 475–483.
Maysami, S., Lan, J.Q., Minami, M., Simon, R.P., 2008. Proliferating progenitor cells: a required cellular element for induction of ischemic tolerance in the brain. J. Cereb. Blood Flow Metab. 28, 1104–1113.
Miki, K., Ishibashi, S., Sun, L., Xu, H., Ohashi, W., Kuroiwa, T., Mizusawa, H., 2009. Intensity of chronic cerebral hypoperfusion determines white/gray matter injury and cognitive/motor dysfunction in mice. J. Neurosci. Res. 87, 1270–1281.
Miyakawa, T., Yamada, M., Duttaroy, A., Wess, J., 2001. Hyperactivity and intact hippocampus-dependent learning in mice lacking the M1 muscarinic acetylcholine receptor. J. Neurosci. 21, 5239–5250.
Morris, R., 1984. Developments of a water-maze procedure for studying spatial learning in the rat. J. Neurosci. Methods 11, 47–60.
Mukherjee, A., Martin, S.G., 2008. The thioredoxin system: a key target in tumour and endothelial cells. Br. J. Radiol. 81, S57–S68. Spec. No 1.
Naylor, A.S., Bull, C., Nilsson, M.K., Zhu, C., Bjork-Eriksson, T., Eriksson, P.S., Blomgren, K., Kuhn, H.G., 2008. Voluntary running rescues adult hippocampal neurogenesis after irradiation of the young mouse brain. Proc. Natl. Acad. Sci. U. S. A. 105, 14632–14637.
Okano, H., Sakaguchi, M., Ohki, K., Suzuki, N., Sawamoto, K., 2007. Regeneration of the central nervous system using endogenous repair mechanisms. J. Neurochem. 102, 1459–1465.
Olsson, T., Hansson, O., Nylandsted, J., Jaattela, M., Smith, M.L., Wieloch, T., 2004. Lack of neuroprotection by heat shock protein 70 overexpression in a mouse model of global cerebral ischemia. Exp. Brain Res. 154, 442–449.
Palmer, T.D., Willhoite, A.R., Gage, F.H., 2000. Vascular niche for adult hippocampal neurogenesis. J. Comp. Neurol. 425, 479–494.
Peng, Y., Feng, S.F., Wang, Q., Wang, H.N., Hou, W.G., Xiong, L., Luo, Z.J., Tan, Q.R., 2010. Hyperbaric oxygen preconditioning ameliorates anxiety-like behavior and cognitive impairments via upregulation of thioredoxin reductases in stressed rats. Prog. Neuropsychopharmacol. Biol. Psychiatry 34, 1018–1025.
Raber, J., Fan, Y., Matsumori, Y., Liu, Z., Weinstein, P.R., Fike, J.R., Liu, J., 2004. Irradiation attenuates neurogenesis and exacerbates ischemia-induced deficits. Ann. Neurol. 55, 381–389.
Ramirez-Ruiz, B., Marti, M.J., Tolosa, E., Bartres-Faz, D., Summerfield, C., Salgado-Pineda, P., Gomez-Anson, B., Junque, C., 2005. Longitudinal evaluation of cerebral morphological changes in Parkinson's disease with and without dementia. J. Neurol. 252, 1345–1352.
Rehni, A.K., Bhateja, P., Singh, N., 2009. Diethyl dithiocarbamic acid, a possible nuclear factor kappa B inhibitor, attenuates ischemic postconditioning-induced attenuation of cerebral ischemia-reperfusion injury in mice. Can. J. Physiol. Pharmacol. 87, 63–68.
Ruiz de Almodovar, C., Lambrechts, D., Mazzone, M., Carmeliet, P., 2009. Role and therapeutic potential of VEGF in the nervous system. Physiol. Rev. 89, 607–648.
Schmidt-Hieber, C., Jonas, P., Bischofberger, J., 2004. Enhanced synaptic plasticity in newly generated granule cells of the adult hippocampus. Nature 429, 184–187.

Shen, Q., Goderie, S.K., Jin, L., Karanth, N., Sun, Y., Abramova, N., Vincent, P., Pumiglia, K., Temple, S., 2004. Endothelial cells stimulate self-renewal and expand neurogenesis of neural stem cells. Science 304, 1338–1340.

Shimazaki, T., Okano, H., 2008. [Mammalian neural stem cells]. Tanpakushitsu Kakusan Koso 53, 311–317.

Shioda, N., Han, F., Fukunaga, K., 2009. Role of Akt and ERK signaling in the neurogenesis following brain ischemia. Int. Rev. Neurobiol. 85, 375–387.

Song, J.S., Cho, H.H., Lee, B.J., Bae, Y.C., Jung, J.S., 2011. Role of thioredoxin 1 and thioredoxin 2 on proliferation of human adipose tissue-derived mesenchymal stem cells. Stem Cells Dev. 20, 1529–1537.

Squire, L.R., 1992. Memory and the hippocampus: a synthesis from findings with rats, monkeys, and humans. Psychol. Rev. 99, 195–231.

Tajiri, S., Oyadomari, S., Yano, S., Morioka, M., Gotoh, T., Hamada, J.I., Ushio, Y., Mori, M., 2004. Ischemia-induced neuronal cell death is mediated by the endoplasmic reticulum stress pathway involving CHOP. Cell Death Differ. 11, 403–415.

Tao, L., Gao, E., Hu, A., Coletti, C., Wang, Y., Christopher, T.A., Lopez, B.L., Koch, W., Ma, X.L., 2006. Thioredoxin reduces post-ischemic myocardial apoptosis by reducing oxidative/nitrative stress. Br. J. Pharmacol. 149, 311–318.

Tschopp, O., Yang, Z.Z., Brodbeck, D., Dummler, B.A., Hemmings-Mieszczak, M., Watanabe, T., Michaelis, T., Frahm, J., Hemmings, B.A., 2005. Essential role of protein kinase B gamma (PKB gamma/Akt3) in postnatal brain development but not in glucose homeostasis. Development 132, 2943–2954.

van Praag, H., Kempermann, G., Gage, F.H., 1999. Running increases cell proliferation and neurogenesis in the adult mouse dentate gyrus. Nat. Neurosci. 2, 266–270.

van Praag, H., Schinder, A.F., Christie, B.R., Toni, N., Palmer, T.D., Gage, F.H., 2002. Functional neurogenesis in the adult hippocampus. Nature 415, 1030–1034.

Wang, L., Andersson, S., Warner, M., Gustafsson, J.A., 2001. Morphological abnormalities in the brains of estrogen receptor beta knockout mice. Proc. Natl. Acad. Sci. U. S. A. 98, 2792–2796.

Wang, B., Gao, Y., Xiao, Z., Chen, B., Han, J., Zhang, J., Wang, X., Dai, J., 2009. Erk1/2 promotes proliferation and inhibits neuronal differentiation of neural stem cells. Neurosci. Lett. 461, 252–257.

Wei, L., Fraser, J.L., Lu, Z.Y., Hu, X., Yu, S.P., 2012. Transplantation of hypoxia preconditioned bone marrow mesenchymal stem cells enhances angiogenesis and neurogenesis after cerebral ischemia in rats. Neurobiol. Dis. 46, 635–645.

Welsh, S.J., Bellamy, W.T., Briehl, M.M., Powis, G., 2002. The redox protein thioredoxin-1 (Trx-1) increases hypoxia-inducible factor 1alpha protein expression: Trx-1 overexpression results in increased vascular endothelial growth factor production and enhanced tumor angiogenesis. Cancer Res. 62, 5089–5095.

West, M.J., Coleman, P.D., Flood, D.G., Troncoso, J.C., 1994. Differences in the pattern of hippocampal neuronal loss in normal ageing and Alzheimer's disease. Lancet 344, 769–772.

Wojtowicz, J.M., Kee, N., 2006. BrdU assay for neurogenesis in rodents. Nat. Protoc. 1, 1399–1405.

Wu, C., Zhan, R.Z., Qi, S., Fujihara, H., Taga, K., Shimoji, K., 2001. A forebrain ischemic preconditioning model established in C57Black/Crj6 mice. J. Neurosci. Methods 107, 101–106.

Yoshioka, H., Niizuma, K., Katsu, M., Okami, N., Sakata, H., Kim, G.S., Narasimhan, P., Chan, P.H., 2011. NADPH oxidase mediates striatal neuronal injury after transient global cerebral ischemia. J. Cereb. Blood Flow Metab. 31, 868–880.

Zhang, R., Zhang, Z., Zhang, C., Zhang, L., Robin, A., Wang, Y., Lu, M., Chopp, M., 2004. Stroke transiently increases subventricular zone cell division from asymmetric to symmetric and increases neuronal differentiation in the adult rat. J. Neurosci. 24, 5810–5815.

Zhang, H.P., Yuan, L.B., Zhao, R.N., Tong, L., Ma, R., Dong, H.L., Xiong, L., 2010. Isoflurane preconditioning induces neuroprotection by attenuating ubiquitin-conjugated protein aggregation in a mouse model of transient global cerebral ischemia. Anesth. Analg. 111, 506–514.

Zhang, R.L., Chopp, M., Roberts, C., Jia, L., Wei, M., Lu, M., Wang, X., Pourabdollah, S., Zhang, Z.G., 2011. Ascl1 lineage cells contribute to ischemia-induced neurogenesis and oligodendrogenesis. J. Cereb. Blood Flow Metab. 31, 614–625.